Arch. Metall. Mater. **68** (2023), 3, 1035-1040

DOI: https://doi.org/10.24425/amm.2023.145472

L.W. KEONG[1], F.F. ZAINAL[1], M.Z. KASMUIN[1], A.A. MOHAMAD[2],
M.F.M. NAZERI[1], M. NABIAŁEK[3], B. JEŻ[4]

WETTABILITY AND HARDNESS INVESTIGATION OF NICKEL-COATED PRECIPITATED CALCIUM CARBONATE Sn-9Zn COMPOSITE SOLDER

To fabricate a lead-free solder with better properties, a surface-modified precipitate calcium carbonate (PCC) was added as a reinforcement phase to tin-zinc (Sn-9Zn) solder. The surface modification of PCC was done by using electroless plating to deposit nickel (Ni) layer on the PCC. Based on microstructure analysis, a thin layer of Ni was detected on the reinforcement particle, indicating the Ni-coated PCC was successfully formed. Next, composite solder of Sn-9Zn-xNi-coated PCC (x = 0, 0.25, 0.50, 1.00 wt.%) was prepared. The morphology and phase changes of the composite solder were evaluated by using optical microscope and X-ray diffraction (XRD). Significant refinement on the grain size of Zn was seen with the additions of Ni-coated PCC, with a new phase of Ni_3Sn_4 was detected along with the phases of Sn and Zn. The wettability of Sn-9Zn was also improved with the presence of Ni-coated PCC, where the wetting angle decreased from 28.3° to 19.4-23.2°. Brinell hardness test revealed up to 27.9% increase in hardness for the composite solder than the pristine Sn-9Zn solder. This phenomenon contributed by the increased in dislocation resistance through Zener pinning effect and Zn grain refinement within the composite solder which enhanced the overall properties of the composite solder.

Keywords: Lead-free solder; Composite solder; Sn-9Zn; Precipitate calcium carbonate; Nickel coating

1. Introduction

Lead (Pb)-free solder alloys such as tin-copper (Sn-Cu), tin-silver-copper (Sn-Ag-Cu) and tin-zinc (Sn-Zn) are widely investigated in order to replace the toxic Sn-Pb alloys. The eutectic Sn-9Zn gained popularity due to its relatively cheap price, high availability and excellent mechanical properties [1,2]. Besides that, it's low melting temperature of 199°C was comparable with the binary eutectic Sn-37Pb that enables the use of Sn-9Zn in the existing production lines with minor alterations. However, the Sn-9Zn solder had scarcely used in electronic packaging due to the low oxidation resistance attributed by to the presence of active Zn phase hindering the wettability of this solder [3]. Therefore, a novel of Sn-9Zn lead-free solders with high better wettability is required.

Two main methods to enhance the Pb-free solder performance are through the microalloying approach [4], or the formation of composite solder by adding non-interacting ceramic reinforcements. In recent years, the formation of composite solder is becoming more favorable. Various type of ceramic particles has been tried as reinforcement, with the justification of selecting the type of ceramics rest on specific factors such as special intended structure, compatibility of synthesizing techniques and cost.

Ceramics such as titanium dioxide (TiO_2) [5] and carbon nanotubes [6] have shown various level of success in improving Pb-free solders. For example, the additions of ceramic able to improve mechanical properties through microstructure refinement [7], enhanced shear stress properties through the additions of alumina [8] and smaller thickness of intermetallic compound (IMC) were seen for the titanium oxide/Sn-3.0Ag-0.5Cu solder system [9]. Precipitated calcium carbonate (PCC) had the potential to be used as ceramic filler in composite. PCC has been used as the filler in many industries to enhance the material properties

[1] UNIVERSITI MALAYSIA PERLIS (UNIMAP),CENTER OF EXCELLENCE GEOPOLYMER & GREEN TECHNOLOGY (CEGEOGTECH 02600, ARAU, PERLIS, MALAYSIA
[2] UNIVERSITI SAINS MALAYSIA, SCHOOL OF MATERIALS AND MINERAL RESOURCES ENGINEERING, ADVANCED SOLDERING MATERIALS GROUP, 14300 NIBONGTEBAL, PENANG, MALAYSIA
[3] CZĘSTOCHOWA UNIVERSITY OF TECHNOLOGY, FACULTY OF PRODUCTION ENGINEERING AND MATERIALS TECHNOLOGY, DEPARTMENT OF PHYSICS, 19 ARMII KRAJOWEJ AV., 42-200 CZĘSTOCHOWA, POLAND
[4] CZESTOCHOWA UNIVERSITY OF TECHNOLOGY, FACULTY OF MECHANICAL ENGINEERING AND COMPUTER SCIENCE, DEPARTMENT OF TECHNOLOGY AND AUTOMATION, L9C ARMII KRAJOWEJ AV., 42-200 CZESTOCHOWA, POLAND

* Corresponding author: firdausnazeri@unimap.edu.my

due to its shape and texture, which are compatible with other materials [10]. Furthermore, it is known that PCC was highly filler retention and had low optical properties compared to other reinforced particle-like titanium and alumina [11].

However, serious phase segregation was widely reported to be encountered while producing composite solder. The Van der Waals force has been identified as one of the contributing factors in the formation of aggregated ceramic particles. This leads to the poor dispersion of the reinforcement phase and resulted in phase segregation of composite components [12]. Worse, stark contrast in density between the ceramic reinforcement and its solder alloy matrix counterparts also making the uniform dispersion difficult [12]. To overcome this issue, surface modifications on the ceramic particles can be done. Electroless plating is a versatile coating technique that is widely used to coat non-electrically conductive surface. Metals such as gold [13], palladium [14] and Ni [15] can be deposited by using this technique. By introducing coating metal layer on the ceramic filler, interfacial bridging can be introduced and possibly improve the distribution of the reinforcement phase in the solder matrix. Nickel is an ideal choice of coating materials to be used as interfacial bridging material. Thin layer of Ni coating has been reported to successfully reduce graphene nanosheets aggregation in Pb-free solder [16]. Besides that, Ni is also known to effectively minimize the eutectic region in graphene-SAC305 solder [17]. The prospect of producing composite solder with improved performance the combination of Ni layer, PCC and Sn-9Zn is good, but are yet to be investigated.

In this work, the effect of Ni coating on PCC and its impact on the wettability and hardness of Sn-9Zn will be investigated, specifically at different content of reinforcement phase loading. To support the findings, basic characterization such as microstructure, elemental changes and phase evolution will be done.

2. Experimental

PCC (Sigma-Aldrich) was used as the reinforcement with an average 5-20 um length. Nickel chloride and sodium hypophosphite solution were obtained from Wako Pure Chemical Industries, Ltd. Pure Sn and Zn were used as raw materials to produce the master binary Sn-9Zn alloy.

Distilled water was prepared and heated to 80°C. After that, nickel chloride (NiCl2.6H2O) (varied at 1%, 5%, and 10%) and 20 g of calcium carbonate CaCO3 were added into the heated distilled water, and the mixture was stirred at 400 rpm. While maintaining the temperature, a few drops of sodium hydroxides (NaOH) was added into the bath solution to get pH 8. Next, sodium hypophosphite (NaH_2PO_2) will be added at 1%, 5% and 10% (ratio1:1 with $NiCl_2$. $6H_2O$). The $NiCl_2$. $6H_2O$ acts as a reducing agent to reduce the Ni ion. After 2 hours, the slurry was obtained by filtering out from the bath solution and dried overnight in the oven at 70°C. The dried residue was crushed into powder using a mortar and pestle. X-ray diffraction (XRD, Ultima IV, Rigaku, Japan) analyzed the raw and modified PCC phase. Ni-PCC microstructural and element analysis were characterized using Scanning electron microscopy (SEM, Hitachi S4000) equipped with energy-dispersive spectroscopy (EDS).

Pure Sn (Malaysia Smelting) and Zn (Sigma-Aldrich) will be used as raw materials to produce the master alloy of binary Sn-9Zn solder. Appropriate amounts of the metals will be cleaned, weighed, and co-melted in a porcelain crucible using an induction furnace at 600°C in the presence of nitrogen (N_2) gas. The molten solder is thoroughly agitated during melting to ensure homogenization. The produced binary Sn-9Zn solder was cast and air-cooled to room temperature.

A portion of the binary Sn-9Zn solder will be remelted at 300°C in N_2 gas. Next, add the Ni-PCC was added into the molten Sn-9Zn solder based on the composition shown in TABLE 1. The mixture was stirred by using a glass rod to make sure the reinforcement is mixed equally. After that, the molten composite solder was cast and cooled to room temperature. Next, a two-roll mill was used to roll the solid solder into a sheet form. A puncher was used to punch the solder sheet to get a small circle shape of solder with a thickness of 3 mm and 5 diameters. The produced pellet was ground, polished, and cleaned. After that, XRD (Shimadzu XRD 6000) and optical microscope (Olympus BX50) were used to analyze the phase and microstructure of the samples. All mounted samples were ground, polished, and cleaned with water prior characterizations. The grain size of the samples was measured by using ImageJ software. Hardness tests were conducted using a Digital Brinell Rockwell Hardness. The wettability was evaluated by measuring the wetting angles on the cross-sectioned solder after reflowing process on Cu substrate at 250°C.

TABLE 1

Composition of the composite solder

Sn-9Zn weight percentage (wt.%)	5 wt.% Ni-PCC reinforcement loading weight percentage (wt.%)
100.00	0.00
99.75	0.25
99.50	0.50
99.00	1.00

3. Results and Discussions

3.1. Surface modification of PCC

The microstructure of PCC exhibits a tetrahedral shape with an average length of 1 to 2 um (Fig. 1a). The PCC surface was smooth and without impurities attached to the surface, as indicated by the elemental analysis that PCC was made of Ca, C and O (TABLE 2). For the modified PCC, the shape of the PCC was maintained, with presence of nickel particles coating now can be detected (Fig. 1b-d), as lowest elemental Ni percentage detected for the 1 wt.% Ni coating. During electroless plating, precursor of sodium hypophosphite underwent a reduction process and released a hydrogen atom that attached to the

TABLE 2

EDX results for raw PCC and Ni-PCC

Sample	C (wt.%)	O (wt.%)	Ca (wt.%)	Ni (wt.%)	Au (wt.%)
PCC coated 0% Nickel	25.24	56.32	12.98	—	5.46
PCC coated 1% Nickel	18.50	65.48	14.23	1.08	0.72
PCC coated 5% Nickel	19.18	60.25	18.38	1.59	0.61
PCC coated 10% Nickel	29.64	40.81	26.93	2.26	0.36

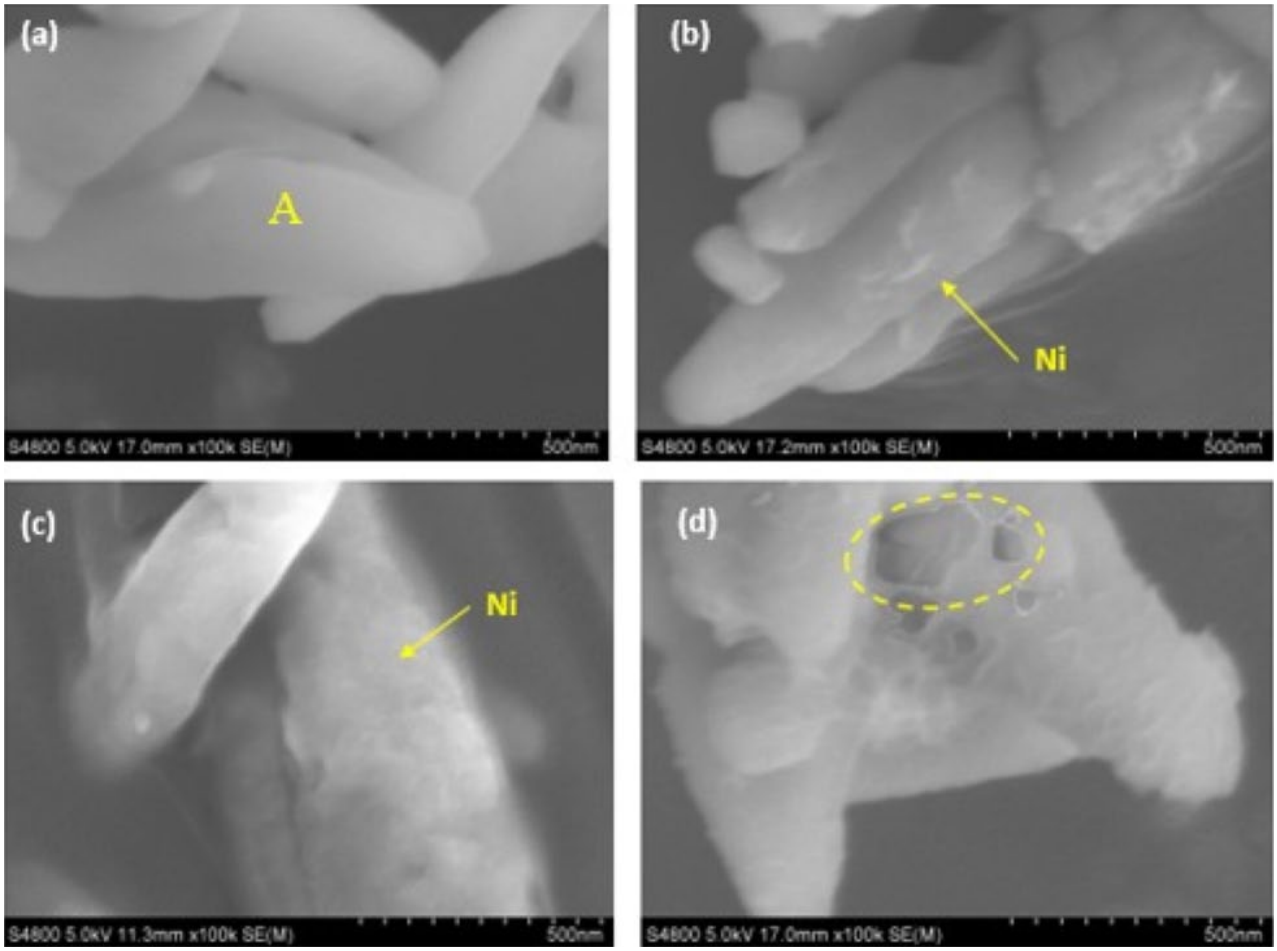

Fig. 1. SEM images of Ni-PCC at 100 000× magnification with different Ni percentage: (a) 0%, (b) 1%, (c) 5%, and (d) 10%

PCC surface (Fig. 2). Next, Ni^{2+} ion from nickel chloride and hypophosphite ion underwent reduction process, producing Ni atom to produce coating layer [18].

At low Ni composition of 1 wt.%, the presence of Ni coating was very minimal, with most of the surface PCC particles was remained exposed. As the Ni percentage increased to 5 wt.%, the coating was evenly distributed on the surface of the PCC, covering most of the surface. Good coating coverage at 5 wt.% of Ni was the same as prepared by another researcher [19]. At 10 wt.% of Ni coating, aggregation and inconsistent thickness was observed. This indicate that at 10 wt.%, excessive Ni coating was produced that may degrade the coating properties, or produce non-uniform performance [20]. As a result, 5 wt.% Ni is seen as the best composition to ensure conformity of the coating is achieved, and the subsequent composite solder assessment will be done by using this composition.

3.2. Phase identification

The XRD pattern of raw PCC showed several sharp peaks at 24.0, 29.0, 35.0, 47.5, 56.6, 62.4, 62.8, and 65.0° for calcium carbonate (ICDD 01072-1937) as shown in Fig. 2a. The detected peaks were strikingly similar with previous report [9]. Detection of multiple characteristic peaks of Ni was evident of successfully deposition on the surface on the PCC as a surface modification process. Comparable finding was also reported where main peak of Ni was seen at 45° [21].

The Sn-9Zn solder was identified with peaks of Sn (ICDD 00-001-0926) and Zn (ICDD 00-001-1238). The Sn peak appeared at 31.05, 31.30, 44.29, 44.42, 63.08, 65.11, 72.75, 79.82° and Zn peak appeared at 43.79, 54.82, 82.48°. No new intermetallic phase was detected for this alloy due to limited solubility of each element in each other [22]. Meanwhile, Sn-9Zn with the

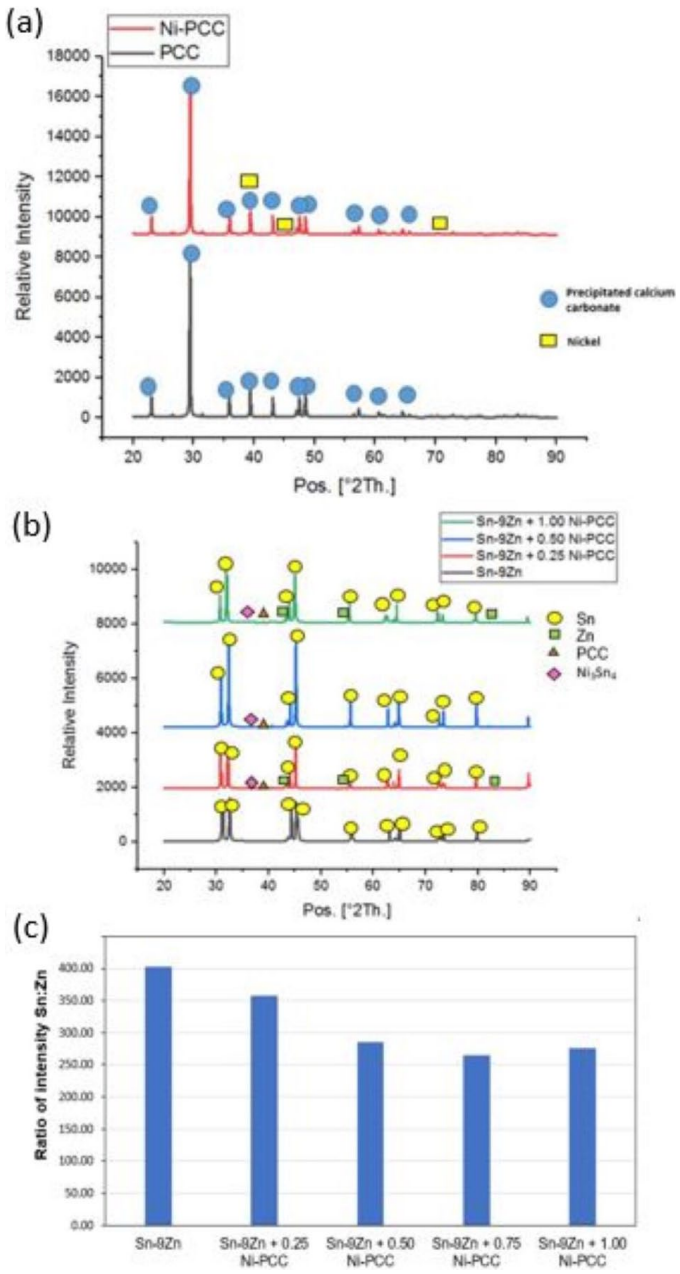

Fig. 2. (a) X-ray diffraction of plain PCC and Ni-PCC; (b) XRD curve composite solder Sn-9Zn + xNi-PCC (x = 0.25, 0.50 & 1.00 wt.%; (c) ratio intensity of Sn to Zn of Sn-9Zn and composite solder Sn-9Zn + x Ni-PCC (x = 0.25, 0.50 & 1.00 wt.%)

addition of 5% Ni-PCC at different loading percentages showed additional peaks for Ni_3Sn_4 (ICDD 03-065-4310) and PCC. The existence of this intermetallic compound highlights that Sn reacted with Ni to produce new compound [9].

In order to evaluate the 5% Ni-PCC additions effect to the Sn-9Zn matrix, the XRD peak intensity ratio of Sn (101) to Zn (002) was calculated based different reinforcement loading (Fig. 3c). The result shows that as the Ni-PCC content increased, the ratio of peak intensity of Sn to Zn was reduced. This can be explained that amount of primary Zn phase was rising in the β-Sn matrix, attributed by the precipitation process [23]. The Ni-PCC reinforcement particle acted as heterogeneous nucleation sites of Zn phase which may help in the precipitation process.

3.3. Microstructure Analysis

The microstructure of Sn-9Zn consisted of β-Sn matrix with distributed needle-like Zn grains (Fig. 3a). This is consistent with the XRD analysis where only two phases were detected for Sn-9Zn. The size of Zn phase was reduced as 5% Ni-PCC was loaded up to 0.5 wt.% (Fig. 3b). The reduction in size were about 2.21, 1.13 and 1.35 μm for 0.25, 0.50 and 1.00 wt.%, respectively. The smallest Zn grain size was seen at the loading of 0.5 wt.% which significantly refined as compared to pristine Sn-9Zn solder (3.47 μm). The results indicate that the addition of Ni-PCC was able to suppress the growth of Zn phase. It can be inferred that the refinement effect by Ni-PCC additions is due to Zener pinning effect that inhibits the growth of grain size [12]. At the same time, the presence of Ni-PCC during solidi-

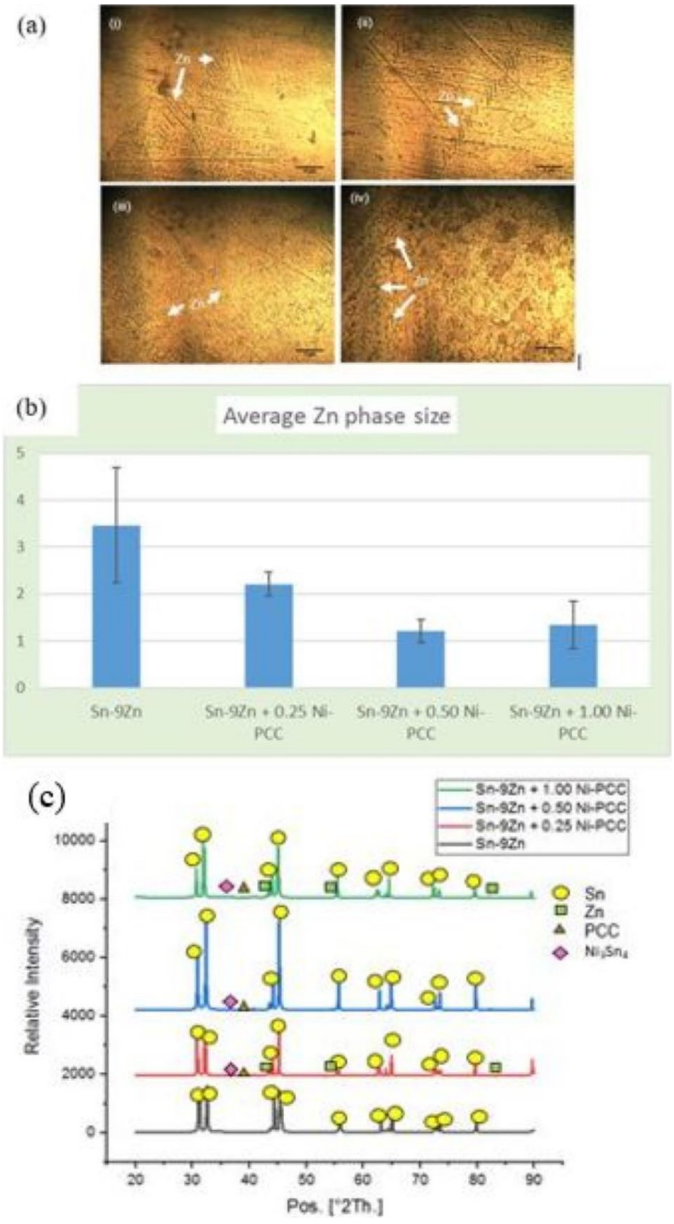

Fig. 3. (a) Microstructure of composite solder Sn-9Zn + xNi-PCC (i) x = 0, (ii) x = 0.25, (iii) x = 0.50, (iv) x = 1.00 wt.%; (b) Average size of Zn phase of composite solder Sn-9Zn + xNi-PCC (x = 0, 0.25, 0.50 & 1.00 wt.%)

fication of Sn-9Zn acted as the heterogeneous nucleation sites that allows solidification process to start without needing high undercooling temperature. This allows solidification of smaller grains compared with homogenous nucleation.

3.4. Wettability evaluation

The average contact angle of the Sn-9Zn solder was 28.3°, which was reduced to 19.4-23.2° after the addition of Ni-PCC (Fig. 4). The lowest contact angle was recorded for the Sn-9Zn-0.5Ni-PCC (19.4°). This result indicated that the wettability was enhanced with the presence of Ni-PCC. This result is comparable with Xu et al. [24], where the solder contact angle reducing as reinforced particle incorporated in solder. The reduction of wetting angle was related to an interfacial reaction between copper substrate and molten solder.

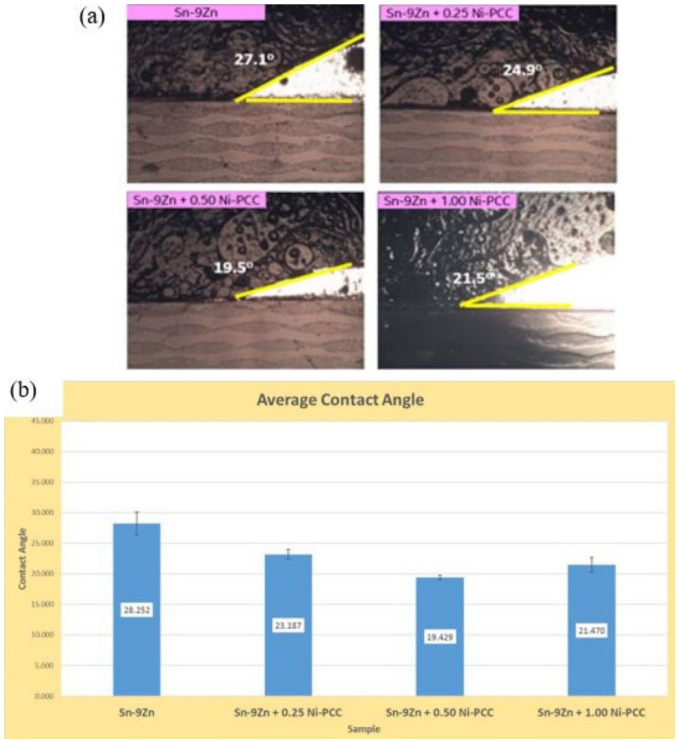

Fig. 4. (a) Image of contact angle of composite solder Sn-9Zn + xNi-PCC (x = 0.25, 0.50 & 1.00 wt.%); (b) Average contact of composite solder Sn-9Zn + xNi-PCC (x = 0.25, 0.50 & 1.00 wt.%)

The Ni-PCC possibly inhibit the growth of the Zn phase that causes an increase in the surface energy. This created a difference in surface energy gradient which elevate the instability and speed up the interfacial during the solder melting process which was beneficial to the spreading of molten solder in the copper plate. Furthermore, the reinforcement phase remained solid state during melting process, which improved the wettability through capillary action [25]. Said et al. [26] stated that the wetting angle less than 60° considered acceptable in the electronic industry. As a result, sample compositions in this study can be considered having acceptable wettability. However, beyond the additions of 0.5 wt.%, the wetting angle slightly increased to 22.5°, indicating adding higher loading is ineffective in improving the wettability.

3.5. Hardness evaluation

The hardness of pure Sn-9Zn was 15.97 HB at the indentation area of 1.82 mm^2 (Fig. 5). Slight increment to 17.28 and 20.44 HB were seen for 0.25 and 0.50 wt.% reinforcement loading (indentation area of 1.71 and 1.44 mm^2, respectively), indicating better mechanical properties for the composite solder. According to Kim et al. [27]. the enhancement of mechanical properties of composite solder is due to the dislocation process is being halted by the reinforcement when the force was applied. However, as the 5% Ni-PCC content was more than 0.5 wt.%, it is obvious that the HB value started to dip slightly. This is attributed to the slightly larger grain size obtained at 1 wt.% reinforcement loading previously seen in microstructure analysis.

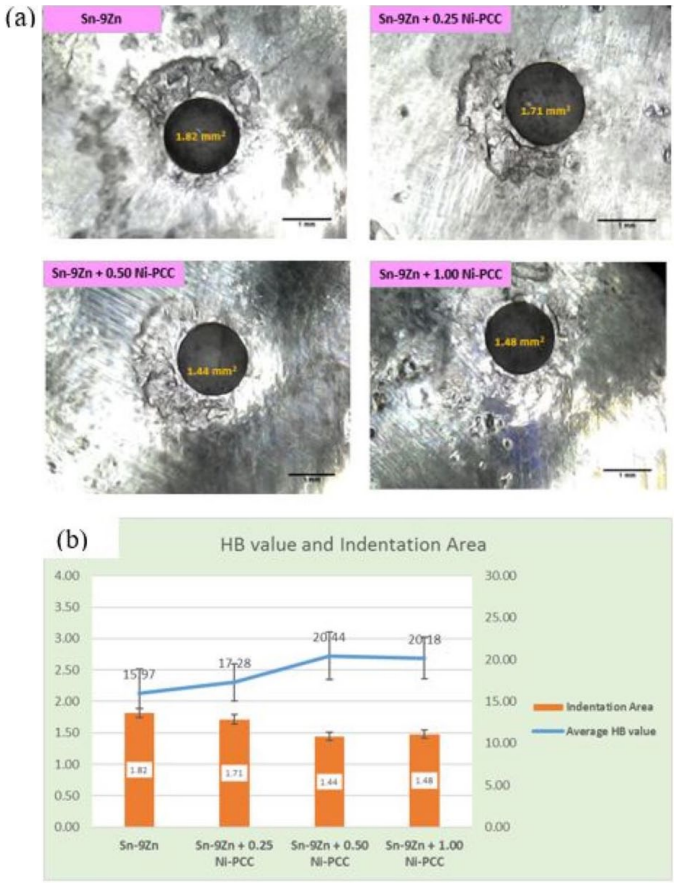

Fig. 5. (a) Image of indentation of composite solder Sn-9Zn + xNi-PCC (x = 0.25, 0.50 & 1.00 wt.%) after Brinell Test; (b) Average HB value and Indentation Area of composite solder Sn-9Zn + x Ni-PCC (x = 0.25, 0.50 & 1.00 wt.%) after Brinell Test

It is widely known that larger grain size produces lower hardness due to less grain boundaries area to impede the dislocation. Thus, it can be summarized that the additions of 0.5 wt.% of 5% Ni-coated PCC produces the optimum hardness for the Sn-9Zn-x Ni-PCC.

4. Conclusion

The main objective of this study is to investigate the enhancement of the wettability and hardness of Sn-9Zn-x Ni-PCC. The coating at 5 wt.% Ni produces the best conformity on the surface of the PCC. It is clear that the additions of Ni-PCC successfully reduce the grain size of Zn phase, while introducing new phases of Ni3Sn4 to the Sn-9Zn. Consequently, smaller grains of Zn and the presence of PCC allow changes in surface energy that reduces the contact angle on copper substrate, highlighting wettability was improved, especially at 0.5 wt.% loading. The optimum hardness can also be seen at 0.5 wt.% loading, due to the impingement of dislocation by the presence of finer grain. It can be concluded that both wettability and hardness of Sn-9Zn were successfully improved by the additions of Ni-PCC.

Acknowledgements

The authors would thank the Ministry of Higher Education Malaysia financial support through the Fundamental Research Grant scheme FRGS/1/2019/TK05/UNIMAP/02/5.

REFERENCES

[1] M.I.I. Ramli, M.A.A.M. Salleh, R.M. Said, M.M.A.B. Abdullah, D.S. Che Halin, N. Saud, M. Nabiałek, Metals **11** (3), 380 (2021). DOI: https://doi.org/10.3390/met11030380

[2] S. Kim, W. Hong, H. Nam, N. Kang, Journal of Welding Joining **39**, 89-102(2021). DOI: https://doi.org/10.5781/JWJ.2021.39.1.11

[3] J. Qiu, Y. Peng, P. Gao, C. Li, J. Materials **14**, 2335 (2021). DOI: https://doi.org/10.3390/ma14092335

[4] P. Xue, K.-H. Wang, Q. Zhou, J. Huang, W.-M. Long, Q.-K. Zhang, Journal of Materials Science: Materials in Electronics **27**, 3742-3747 (2016). DOI: https://doi.org/10.1007/s10854-015-4217-3

[5] S.S.M. Nasir, M.Z. Yahaya, A.M. Erer, B. Illés, A.A. Mohamad, J. Ceramics International **45**, 18563-18571 (2019). DOI: https://doi.org/10.1016/j.ceramint.2019.06.079

[6] N. Ismail, A. Jalar, M.A. Bakar, N.S. Safee, W.Y.W. Yusoff, A. Ismail, J. Soldering Surface Mount Technology **33** (1), 47-56 (2020). DOI: https://doi.org/10.1108/SSMT-11-2019-0035

[7] H. Wang, K. Zhang, C. Yin, M. Zhang, J. Metals **9** 1123 (2019). DOI: https://doi.org/10.3390/met9101123

[8] A. Geranmayeh, R. Mahmudi, M. Kangooie, J. Materials Science Engineering **A 528**, 3967-3972 (2011). DOI: https://doi.org/10.1016/j.msea.2011.02.034

[9] W.K. Leong, A.A. Mohamad, M.F.M. Nazeri, Journal of Physics: Conference Series **2080**p. 012019IOP Publishing, (2021). DOI: https://doi.org/10.1088/1742-6596/2080/1/012019

[10] S.F.A. Ali, M. El Batouti, M. Abdelhamed, E. El-Rafey, J Journal of Materials Research **9** 12840-12854 (2020). DOI: https://doi.org/10.1016/j.jmrt.2020.08.113

[11] F. Munawaroh, L.K. Muharrami, Z. Arifin, KnE Engineering 98-104 (2019). DOI: https://doi.org/10.18502/keg.v1i2.4435

[12] L.W. Keong, A.A. Mohamad, M.F.M. Nazeri, Surface Modifications on Ceramic Reinforcement for Tin-Based Composite Solders, Recent Progress in Lead-Free Solder Technology, Springer 53-75 (2022). DOI: https://doi.org/10.1007/978-3-030-93441-5_3

[13] D. Baudrand, J. Bengston, Metal Finishing **93**, 55-57 (1995). DOI: https://doi.org/10.1016/0026-0576(95)99502-2

[14] Y.S. Cheng, K.L. Yeung, Journal of Membrane Science **182**, 195-203 (2001). DOI: https://doi.org/10.1016/S0376-7388(00)00563-9

[15] Q. Yu, T. Zhou, Y. Jiang, X. Yan, Z. An, X. Wang, D. Zhang, T. Ono, Applied Surface Science **435**, 617-625 (2018). DOI: https://doi.org/10.1016/j.apsusc.2017.11.169

[16] H. Wang, K. Zhang, M. Zhang, J. Journal of Alloys Compounds **781**, 761-772 (2019). DOI: https://doi.org/10.1016/j.jallcom.2018.12.080

[17] S. Li, Y. Liu, H. Zhang, H. Cai, F. Sun, G. Zhang, Results in Physics **11**, 617-622 (2018). DOI: https://doi.org/10.1016/j.rinp.2018.10.005

[18] F.B. Mainier, M.P.C. Fonseca, S.S. Tavares, J.M. Pardal, Journal of Materials Science Chemical Engineering Journal **1**, 1-8 (2013). DOI: http://dx.doi.org/10.4236/msce.2013.16001

[19] F. Huo, Z. Jin, D. Le Han, K. Zhang, H. Nishikawa, J. Materials Design 110038 (2021). DOI: https://doi.org/10.1016/j.matdes.2021.110038

[20] C. Zhang, D. Yao, J. Yin, K. Zuo, Y. Xia, H. Liang, Y.-P. Zeng, J. Materials Design **159**, 117-126 (2018). DOI: https://doi.org/10.1016/j.matdes.2018.08.055

[21] V.K. Yadav, K.K. Yadav, M. Cabral-Pinto, N. Choudhary, G. Gnanamoorthy, V. Tirth, S. Prasad, A.H. Khan, S. Islam, N.A. Khan, J. Applied Sciences **11**, 4212 (2021). DOI: https://doi.org/10.3390/app11094212

[22] M.F.M. Nazeri, A.A. Mohamad, J. Int. J. Electroactive Mater. **2**, 34-39 (2014).

[23] M.M. Billah, K.M. Shorowordi, A. Sharif, Journal of Alloys Compounds **585**, 32-39 (2014). DOI: https://doi.org/10.1016/j.jallcom.2013.09.131

[24] K.-K. Xu, L. Zhang, L.-L. Gao, N. Jiang, L. Zhang, S.-J. Zhong, J. Science Technology of Advanced Materials **21**, 689-711 (2020). DOI: https://doi.org/10.1080/14686996.2020.1824255

[25] R. Sayyadi, F. Khodabakhshi, N.S. Javid, G.J.J.o.M.R. Khatibi, Journal of Materials Research Technology **9**8953-8970 (2020). DOI: https://doi.org/10.1016/j.jmrt.2020.06.026

[26] R.M. Said, N. Saud, M.A.A. Mohd Salleh, M.N. Derman, M.I. Izwan Ramli, N.M. Nasir, Trans. Tech. Publ. **754**, 546-550 (2015). DOI: https://doi.org/10.4028/www.scientific.net/AMM.754-755.546

[27] S.H. Kim, M.-S. Park, J.-P. Choi, C. Aranas Jr, J. Scientific reports **7**1-14 (2017). DOI: https://doi.org/10.1038/s41598-017-14263-6